Application of seaweeds for the removal of cationic dye from aqueous solution

J. Jegan[a,*], J. Vijayaraghavan[a], T. Bhagavathi Pushpa[a], S.J. Sardhar Basha[b]

[a]*Department of Civil Engineering, University College of Engineering Ramanathapuram, Ramanathapuram 623513, Tamil Nadu, India, Tel. +91 9655776622; email: drjeganjoe@gmail.com (J. Jegan), Tel. +91 9488528279; email: vijayaraghavanmalar@gmail.com (J. Vijayaraghavan), Tel. +91 9790437905; email: pushpathillai@gmail.com (T. Bhagavathi Pushpa)*
[b]*Department of Chemistry, University College of Engineering Ramanathapuram, Ramanathapuram 623513, Tamil Nadu, India, Tel. +91 9962573707; email: jsardhar@gmail.com*

ABSTRACT

The removal of a cationic dye (crystal violet) from aqueous solution by two red seaweeds (*Gracilaria edulis* and *Kappaphycus alvarezii*) under different environmental conditions was investigated. Biosorption of crystal violet was studied by varying particle size (0.712–2.36 mm), biomass dosage (2–8 g/L), solution pH (2–9), initial dye concentration (50–1,000 mg/L) and contact time (0–360 min). At optimum seaweed particle size (1.18 mm), seaweed dosage (5 g/L), equilibrium pH (8), initial dye concentration (100 mg/L) and equilibrium time (360 min), *G. edulis* and *K. alvarezii* recorded crystal violet uptakes of 181.0 and 171.9 mg/g, respectively. The kinetic data obtained at different initial crystal violet concentrations indicated that biosorption rate was fast for both seaweeds and the data were successfully modelled using the pseudo-first and pseudo-second-order models. The Langmuir, Freundlich and Redlich–Peterson and Sips models were used to describe the crystal violet isotherm data; of which the Sips model described the isotherm data with high correlation coefficients.

Keywords: Biosorption; Crystal violet; Dye; *Kappaphycus alvarezii*; *Gracilaria edulis*; Seaweed

1. Introduction

Crystal violet (CV) dye, belongs to the triphenyl-methane group, is extensively applied in colouring paper, temporary hair colourant, dyeing cottons and wools [1]. It is also widely applied in animal and veterinary medicine as a biological stain [2]. Hence, spent wastewaters emanating from these processes contain high CV concentrations. Crystal violet is harmful by inhalation, ingestion and skin contact, and has also been found to cause cancer and severe eye irritation to human beings [2,3]. It is also non-biodegradable and can persist in variety of environments [4]; hence its removal from wastewaters before their discharge is essential for environmental safety.

Currently, various physico-chemical methods are used to remove dyes and heavy metals from effluents, including coagulation and flocculation, electrochemical destruction precipitation, chemical oxidation and adsorption using activated carbons [5]. In particular, adsorption has been reported to be efficient and economical for wastewater treatment in order to remove dyes, pigments and other colourants [6]. Granular activated carbon has been used successfully, but it is

cost-prohibitive. This has led to search for cheaper adsorbent substitutes derived from bacterial, fungal and industrial wastes [7–9]. However, these sorbents either involve cost-input pretreatments or they are not abundantly available as wastes. The present report attempts to eliminate such preparatory steps and limitations of availability using two commonly available seaweeds. Marine algae, apart from very few cases [10,11] have not been utilized for the removal of dyes. They are well-established metal biosorbents and are abundantly available in most of the world's oceans. However, their efficiency in dye removal is often questionable and not well researched. Thus, the focus of the present study has to investigate the biosorption potential of two red seaweeds (*Gracilaria edulis* and *Kappaphycus alvarezii*) towards CV.

2. Materials and methods

Two red seaweeds (*G. edulis* and *K. alvarezii*) were collected from the beaches in Mandapam region, Tamil Nadu, India. After collection, the seaweed samples were thoroughly washed with tap water to remove wastes, salt debris and other contaminants. They were subsequently washed with deionized water and then dried in an oven at 70℃ overnight. Biosorbent particles were prepared by grounding the dried red seaweeds in a blender and subsequently sieved to obtain desired particle sizes.

The stock dye solution at desired concentration was prepared by dissolving crystal violet (Sigma–Aldrich, India) in deionized water.

The pH of the CV solution was initially adjusted to the desired value using 0.1 M HCl or 0.1 M NaOH. In all experiments, 0.5 g of red seaweed biomass was contacted with 100 mL of dye solution in 250 mL Erlenmeyer flasks. The contents of the flask were agitated in an incubated rotary shaker at 150 rpm for 6 h at 30℃. Once the equilibrium condition was reached, the suspension was centrifuged at 3,500 rpm for 5 min and the supernatant was analysed in a spectrophotometer (Merck, Spectroquant Phara 300) at 584 nm after appropriate dilution for CV concentration. Kinetic experiments were conducted in similar manner except that the samples were withdrawn at predetermined time intervals.

The amount of CV biosorbed by red marine algae was calculated from the differences between the initial amount of dye added and that left in the supernatant, using the following equation:

$$Q = V(C_0 - C_f)/M \tag{1}$$

where Q is the CV uptake (mg/g), C_0 and C_f are the initial and final CV concentrations in the solution (mg/L), respectively, V is the volume of dye solution (L) and M is the weight of red seaweed added (g).

Four isotherm models were used to describe CV isotherm experimental data as follows:

$$\text{Langmuir model: } Q = \frac{Q_{max} \, b_L \, C_f}{1 + b_L \, C_f} \tag{2}$$

$$\text{Freundlich model: } Q = K_F \, C_f^{1/n_F} \tag{3}$$

$$\text{Redlich–Peterson model: } Q_e = \frac{K_{RP} C_f}{1 + a_{RP} \, C_f^{\beta_{RP}}} \tag{4}$$

$$\text{Sips model: } Q_e = \frac{K_S \, C_f^{\beta_S}}{1 + a_S \, C_f^{\beta_S}} \tag{5}$$

where Q_{max} is the maximum CV uptake (mg/g), b_L is the Langmuir equilibrium coefficient (L/mg), K_F is the Freundlich coefficient $(L/g)^{1/n_F}$, n_F is the Freundlich exponent, K_{RP} is the Redlich–Peterson isotherm coefficient (L/g), a_{RP} is the Redlich–Peterson isotherm coefficient $((L/mg)^{\beta_{RP}}$, and β_{RP} is the Redlich–Peterson model exponent, K_S is the Sips model isotherm coefficient $(L/g)^{\beta_S}$, a_S is the Sips model coefficient $((L/mg)^{\beta_S}$ and β_S is the Sips model exponent.

Two kinetic models were used to represent CV biosorbents kinetics experimental data as follows:

$$\text{Pseudo-first-order model: } Q_t = Q_e(1 - \exp(-k_1 t)) \tag{6}$$

$$\text{Pseudo-second-order model: } Q_t = \frac{Q_e^2 \, k_2 t}{1 + Q_e \, k_2 t} \tag{7}$$

where Q_e is the amount of CV biosorbed at equilibrium (mg/g), Q_t is the amount of CV biosorbed at time t (mg/g), k_1 is the pseudo-first-order rate constant (1/min) and k_2 is the pseudo-second-order rate constant (g/mg min). All the model parameters were evaluated by non-linear regression using Sigma Plot (version 4.0, SPSS, USA) software.

The functional groups on the surface of red seaweed which are responsible for the removal of CV were determined using a Bruker-ATR IR (ACPHA) Fourier Transform IR spectrophotometer (Germany). The samples were prepared in the form of pellets using KBr. To understand the biosorbent surface morphology, the samples prior and after adsorption of CV were dried, coated with thin layer of gold and subsequently analysed using scanning electron microscopy (Hitachi S4800, Japan).

3. Results and discussion

3.1. Influence of particle size

Fig. 1 illustrates the effect of seaweed particle size on CV biosorption at solution pH of 8. Several sizes of seaweed particles were used, which include 0.712, 1.18, 2 and 2.36 mm. For both seaweeds, significant variations in CV uptake capacity were observed at different particle sizes. To be precise, CV biosorption capacity was found to be increased by decreasing the particle size of seaweed [12]. This behaviour may be due to the larger external surface area for biosorption as seaweed particles became smaller. The larger surface area to volume ratios of seaweed particles would increase the availability of exterior surface for CV binding and enhance dye uptake capacity. Although the smallest particle size (0.712 mm) resulted in slightly better CV biosorption performance compared to 1.18 mm particles, the increase in uptake was less than 2.8% compared to 1.18 mm particles. It is also desirable to use rigid and relatively big particles in continuous sorption processes as it can tolerate extreme operating conditions [13]. Considering these aspects, seaweed particle size (1.18 mm) was selected for further experiments.

3.2. Influence of algal dosage

Data obtained from the experiments to study the influence of seaweed dosage are presented in Fig. 2. Seaweed dosages were varied from 2 to 8 g/L. From the analysis of experimental data obtained for two red algal biomasses, it was observed that the CV removal efficiency increased with the increase in seaweed dosage. For instance, CV removal efficiency of *G. edulis* and *K. alvarezii* increased from 58.9 to 94.4% and 39.2 to 88.1%, respectively, when the biomass dosage
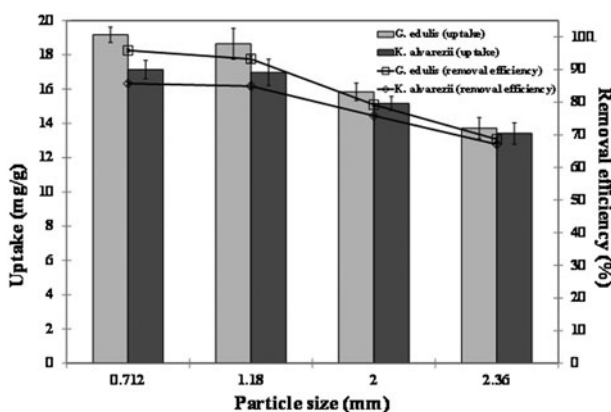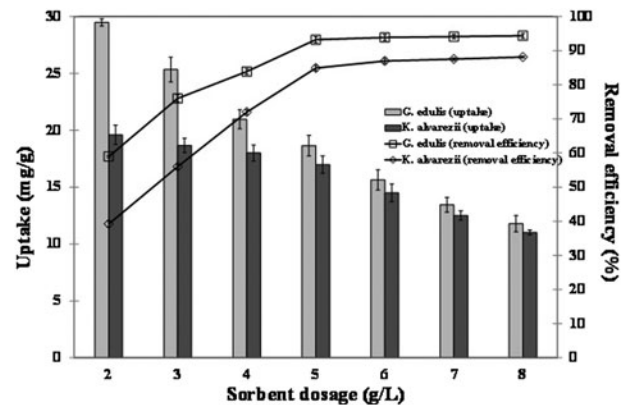
Fig. 2. Effect of seaweed dosage on CV biosorption.

increased from 2 to 8 g/L. The observed increment in removal efficiency with the increase in seaweed dosage could be due to an increase in the number of possible functional groups and surface area of the seaweed biomass [14–16]. On the other hand, the CV uptake decreases on increasing the seaweed dosage. For example, CV uptake capacity of *G. edulis* and *K. alvarezii* decreased from 29.5 to 11.8 mg/g and 19.6 to 11.0 mg/g, respectively, when the biomass dosage increased from 2 to 8 g/L. At low sorbent dosages, the available dye molecules are higher than the amount of binding sites, hence sorptional uptake is higher. In contrary, at high biosorbent dosages, the available dye molecules are insufficient to cover all the exchangeable sites on the seaweed biosorbent usually resulting in low dye uptake. Similar results were obtained in other studies [17,18]. Comparing the % removal efficiency and sorption uptake values, algal dosage of 5 g/L was selected as optimum for further experiments.

3.3. Influence of equilibrium pH and removal mechanism

The pH of wastewater is one of the major parameters controlling the efficiency of biosorption process. Considering this, experiments were conducted at a wide range of pH (2–9). Fig. 3 shows the influence of pH on the CV biosorption capacity of two red seaweeds. The results confirmed that the removal of CV from aqueous solution was strongly influenced by equilibrium pH. Biosorption of CV increased from 3.45 mg/g at pH 2 to 18.6 mg/g at pH 8 for *G. edulis*, whereas 1.98 mg/g observed at pH 2 increased to 16.9 mg/g at pH 8 for *K. alvarezii*. Lower CV uptake at strong acidic pH values is due to the presence of excess H^+ ions in the solution under strong acidic pH conditions [19], which in turn makes the seaweed surface protonated. As the pH increased, the

Fig. 1. Effect of seaweed particle size on CV biosorption.
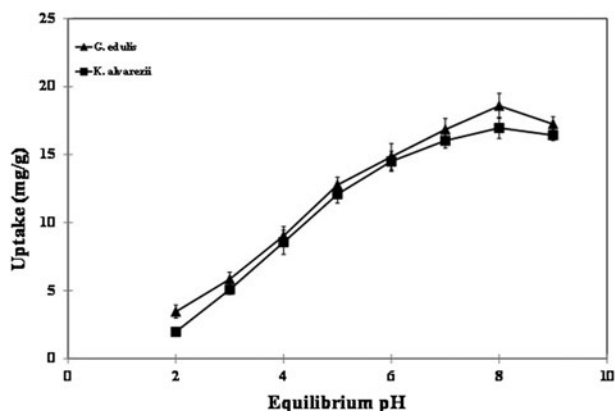
Fig. 3. Effect of equilibrium pH on CV biosorption by *G. edulis* and *K. alvarezii*.

Fig. 4. FT-IR spectra of (a) raw *G. edulis*, (b) CV-loaded *G. edulis*, (c) raw *K. alvarezii* and (d) CV-loaded *K. alvarezii*.

concentration of H^+ ions decreases, which in turn increases the number of negatively charged sites. The surface of the seaweed thus becomes negatively charged, and this increases the biosorption of the positively charged cationic dye molecules through electrostatic forces of attraction. Comparing the extent of removal, *G. edulis* sorbed 8.73% more CV compared to *K. alvarezii*. The influence of pH on biosorption capacity of seaweeds can also be correlated with point of zero charge (pH_{pzc}) of seaweed biomass. The point of zero charge provides information regarding the type of surface active centres and it was determined by solid addition method [20]. The pH_{pzc} of *G. edulis* and *K. alvarezii* biomass were found to be 5.2 and 4.9, respectively. Solution pH values less than pH_{pzc} would result in positively charged biomass [15], resulting in a decreased interaction between the biomass and cationic dyes. Above pH_{pzc}, the biosorbent gets a negative charge and electrostatic interaction between dye molecules and biomass increases which results in high dye removal.

In an effort to understand the nature of functional groups associated with CV biosorption, FT-IR analyses were performed on raw and CV-loaded red seaweed biomasses. As illustrated in Fig. 4, the FT-IR spectrum of raw *G. edulis* and *K. alvarezii* displayed a number of absorption peaks, indicating the complex nature of the biomass. Nevertheless, some characteristic peaks can be assigned for each red alga as illustrated in Table 1 [21,22]. After exposure to CV, significant changes in seaweed functionalities were observed (Fig. 4). This is basically due to the participation of binding groups during interaction with CV and thus causing the changes in the observed wave numbers. In particular, major shifts were observed with asymmetric and symmetric C=O and C–O stretches in CV-loaded samples of red seaweed biomasses on comparison with raw
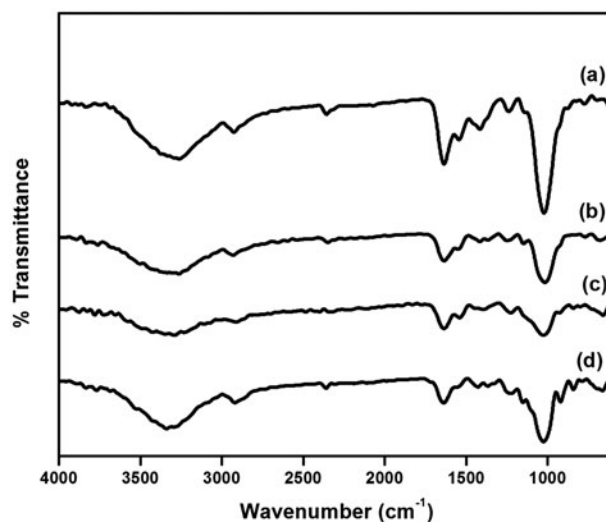
biomasses (Table 1). These results confirm the involvement of negative binding groups on the surface of red seaweed during biosorption of CV molecules.

Fig. 5 illustrates the SEM photographs of raw and CV-loaded red seaweed biomasses. The SEM pictures of both red seaweeds (Fig. 5) revealed surface protuberance and microstructures, which may be due to Ca and other salt crystalloid deposition. After biosorption, the surfaces of *G. edulis* and *K. alvarezii* were covered with CV molecules and hence appeared relatively smooth (Fig. 5).

3.4. Influence of initial CV concentration and kinetics modelling

Biosorption of CV onto *G. edulis* and *K. alvarezii* with respect to contact time was studied within the range of 10–360 min. The initial CV concentration was varied from 50 to 1,000 mg/L at pH 8. The CV biosorption profile at different time intervals has been presented in Figs. 6 and 7. For *G. edulis*, around 90% removal occurred within 50 min for 100 mg CV/L, whereas *K. alvarezii* removed 90% within 60 min. This rapid initial uptake of the CV onto algal biomass is due to the availability of excess vacant sites [23]. As the sorption progresses, binding sites got occupied and less number of vacant sites will be made available on the surface of the adsorbent which results in the decrease in sorption rate as evident in Figs. 6 and 7. After 120 min, the system reached the equilibrium state where there was no significant change in CV concentration in the solution as the available binding sites are occupied by the CV

Table 1
Stretching frequencies observed in raw and CV-loaded red seaweed biomasses [20,21]

Assignment	Wavenumber (cm^{-1})			
	Raw *G. edulis*	CV-loaded *G. edulis*	Raw *K. alvarezii*	CV-loaded *K. alvarezii*
–OH, –NH stretching	3,264	3,262	3,292	3,340
Asymmetric C=O stretch of COOH	1,636	1,634	1,634	1,638
Symmetric C=O	1,415	1,413	1,398	1,428
C–O (COOH) stretch	1,238	1,247	1,226	1,224
C–O (alcohol) band	1,022	1,016	1,028	1,026
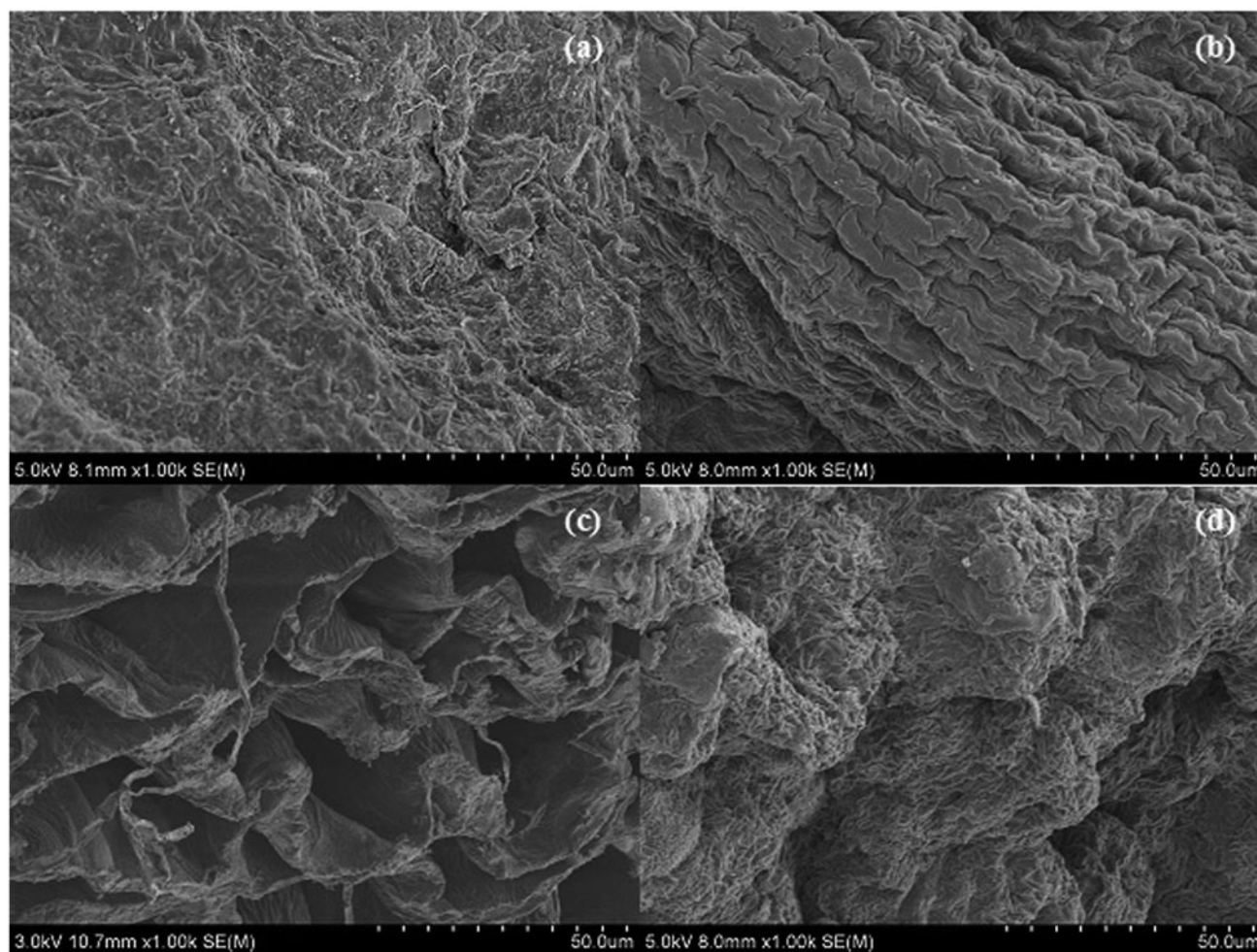
Fig. 5. SEM images of (a) raw *G. edulis*, (b) CV-loaded *G. edulis*, (c) raw *K. alvarezii* and (d) CV-loaded *K. alvarezii*.

molecules. The time taken to attain equilibrium increased with increase in initial CV concentration (Figs. 6 and 7). In general, the equilibrium contact time for CV biosorption onto red seaweeds was found to be 360 min. It is also evident from Fig. 6 that the increase in initial CV concentration improved the CV uptake capacity of both red seaweeds. A higher initial dye concentration was identified to have a higher driving force for transporting cations from ambient liquid to the cell surface, resulting in a faster sequestration and higher adsorption capacity [24]. On increasing initial CV concentration from 50 to 1,000 mg/L, equilibrium CV
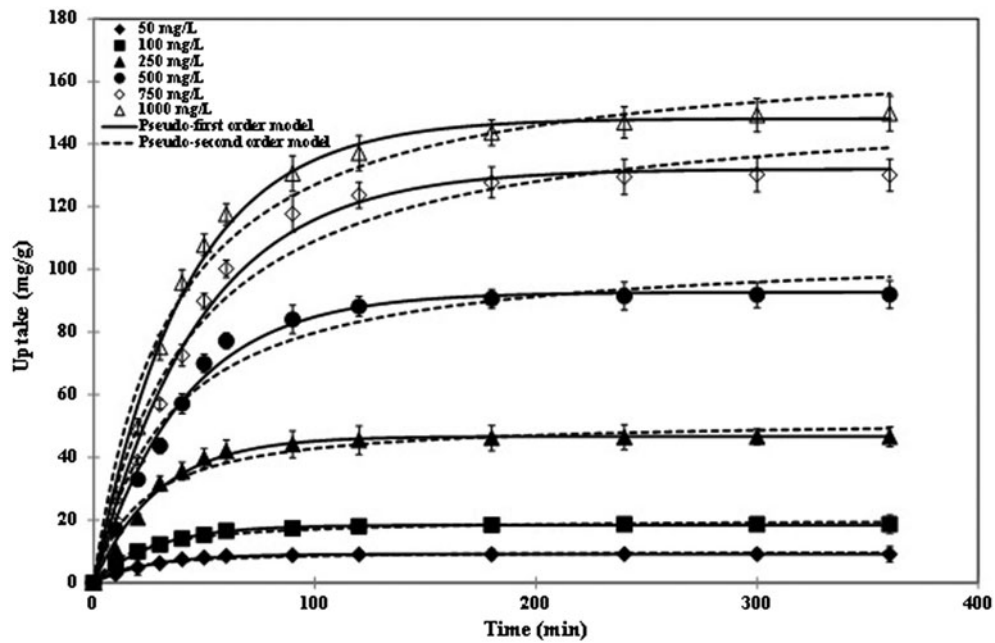
Fig. 6. Biosorption kinetics of CV by *G. edulis*.
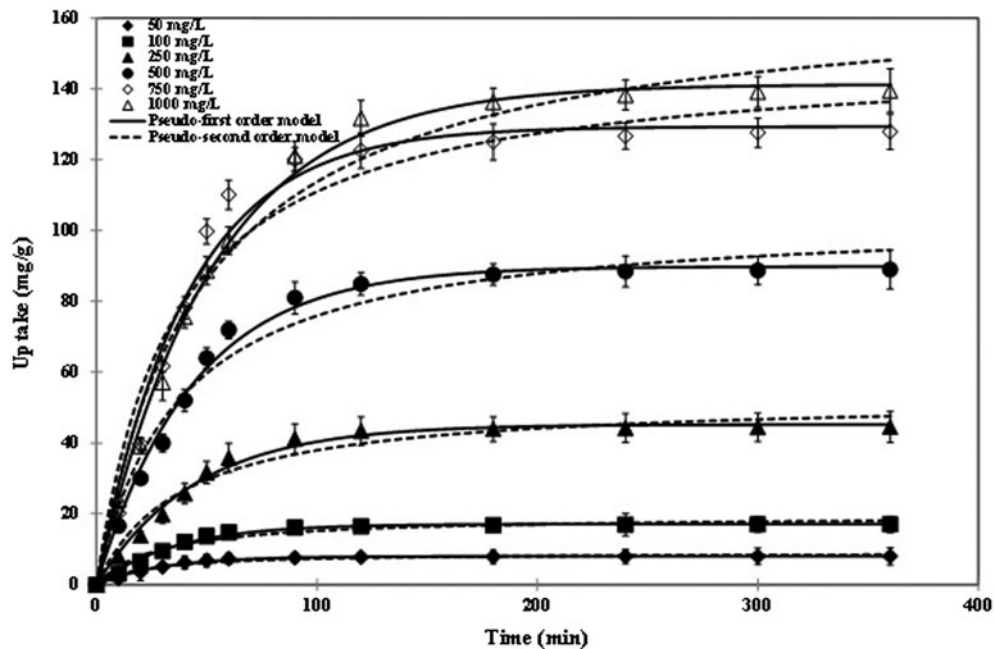
Fig. 7. Biosorption kinetics of CV by *K. alvarezii*.

uptake capacities of *G. edulis* and *K. alvarezii* increased from 9.16 to 149.7 mg/g and 8.01 to 139.5 mg/g, respectively.

The kinetic data of CV onto *G. edulis* and *K. alvarezii* have been examined using the pseudo-first- and pseudo-second-order models. These models were based on the assumption that the rate of biosorption is proportional to the number of vacant binding groups on the surface of the biosorbent, respectively, to the first and second power. Application of CV kinetics data to the pseudo-first-order model resulted in good prediction with high correlation coefficient (R^2) values

(Table 2). The model constants (Q_e and k_1) increased with the increase in initial CV concentration, which indicates that high CV concentration favoured rate and amount of biosorption. Also, the model predicted uptake values close to that of experimental observed values. In the case of pseudo-second-order kinetics, the model over-predicted CV uptake values along with relatively low R^2 values (Table 2). The CV kinetic curves predicted by two models in comparison with experimental kinetics data are presented in Figs. 6 and 7.

3.5. Biosorption isotherm and modelling

Experimental CV biosorption isotherms obtained for *G. edulis* and *K. alvarezii* at pH 8 are plotted in Figs. 8 and 9. Each of these isotherms could be considered as L-shaped [25], i.e. the ratio between the CV concentration in the solution and that biosorbed onto the red seaweed decreases with the increase in CV concentration, providing a concave curve without a strict plateau. Comparing both biosorbents, *G. edulis* exhibited high CV uptake of 149.7 mg/g compared to *K. alvarezii* (139.5 mg/g).

Several two- and three-parameter models were used to analyse experimental CV isotherm data. Application of the Langmuir model to the experimental CV isotherm data provided good R^2 values. The Langmuir isotherm [26] is valid for monolayer adsorption onto a surface comprising a limited number of identical sites [27]. The Langmuir constant, Q_{max}, represents maximum dye uptake values that can be achieved by the system. On the other hand, b_L represents the affinity between the sorbate and biosorbent.
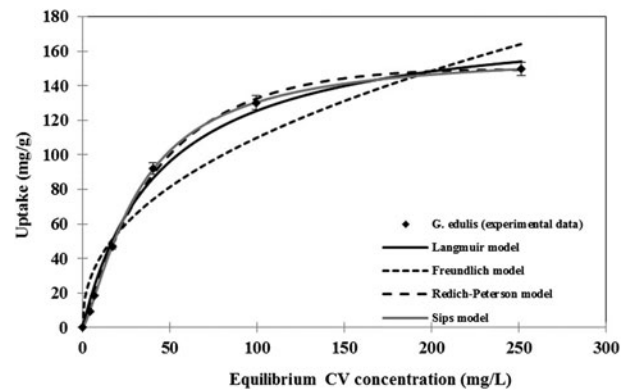
Fig. 8. Biosorption isotherm of CV by *G. edulis*.

Both constants (Q_{max} and b_L) were observed maximum for *G. edulis* compared to *K. alvarezii* (Table 3). Since the Langmuir isotherm model is able to predict the maximum biosorption capacity of any biosorbent under controlled conditions, comparison among sorbent performance towards the particular dye is possible. In that way, efforts were made to compare the CV sorption performance of seaweed species with other sorbents reported in the literature. *Artocarpus heterophyllus* (jackfruit) sorbed 43.4 mg CV/g [28], iron–manganese oxide-coated kaolinite sorbed 20.6 mg CV/g [29], coco-peat sorbed 119.2 mg CV/g [30] and *Ananas comosus* (pineapple) leaf sorbed 158.7 mg CV/g [31] compared to 181.0 and 171.9 mg CV/g exhibited by *G. edulis* and *K. alvarezii*, respectively, in this study.

The Freundlich isotherm [32] was originally empirical in nature, but was later interpreted as sorption to heterogeneous surfaces or surfaces supporting sites of varied affinities. It is assumed that the stronger

Table 2
Kinetic model parameters during biosorption of CV onto *G. edulis* and *K. alvarezii*

Biosorbent	Model		50 (mg/L)	100 (mg/L)	250 (mg/L)	500 (mg/L)	750 (mg/L)	1,000 (mg/L)
G. edulis	Pseudo-first-order	Q_e	9.18	18.4	46.7	92.7	132.0	148.1
		k_1	0.0396	0.0370	0.0342	0.0247	0.0210	0.0242
		R^2	0.998	0.998	0.992	0.992	0.992	0.995
	Pseudo-second-order	Q_e	10.1	20.4	52.2	106.8	155.1	171.1
		k_2	0.0056	0.0026	0.0009	0.0003	0.0002	0.0002
		R^2	0.972	0.990	0.964	0.968	0.970	0.981
K. alvarezii	Pseudo-first-order	Q_e	8.02	17.1	45.2	89.8	129.3	141.3
		k_1	0.0334	0.0285	0.0223	0.0229	0.0245	0.0192
		R^2	0.991	0.991	0.990	0.993	0.982	0.996
	Pseudo-second-order	Q_e	8.98	19.4	52.7	104.3	149.6	167.6
		k_2	0.0049	0.0018	0.0005	0.0003	0.0002	0.0001
		R^2	0.960	0.962	0.965	0.971	0.953	0.979
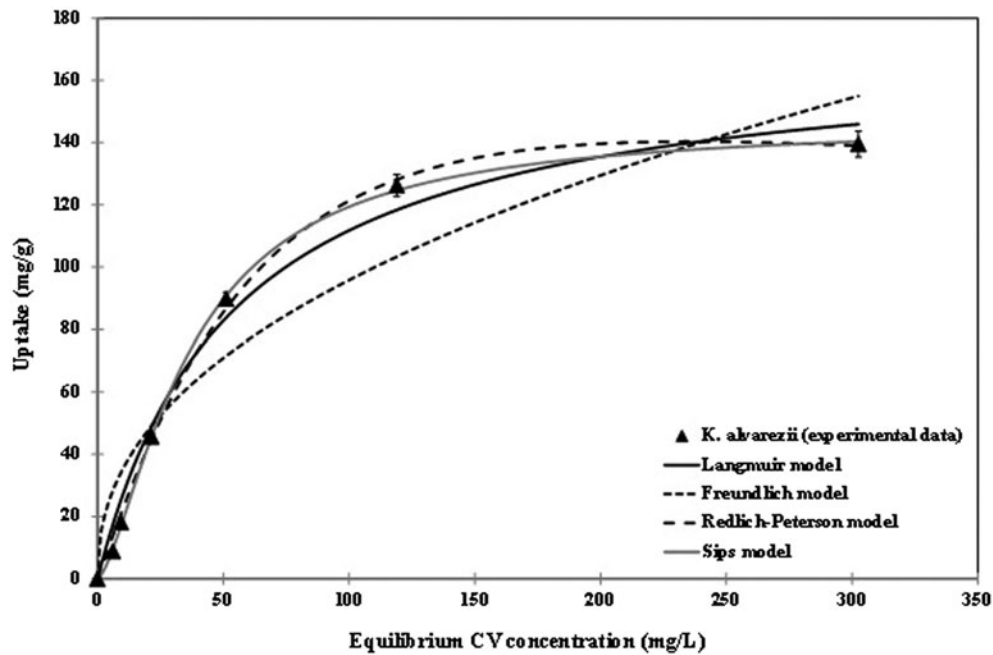
Fig. 9. Biosorption isotherm of CV by *K. alvarezii*.

Table 3
Isotherm model parameters during biosorption of CV onto *G. edulis* and *K. alvarezii*

Models		*G. edulis*	*K. alvarezii*
Langmuir	Q_{max}	181.0	171.9
	b_L	0.0226	0.0186
	R^2	0.993	0.986
Freundlich	K_F	14.8	13.0
	n_F	2.29	2.30
	R^2	0.929	0.911
Redlich–Peterson	K_{RP}	3.23	2.34
	a_{RP}	0.0051	0.0019
	β_{RP}	1.22	1.34
	R^2	0.998	0.997
Sips	K_S	1.54	0.715
	a_S	0.0097	0.0049
	β_S	1.34	1.48
	R^2	0.999	0.999

functional groups are occupied first and the binding strength decreases with the increasing degree of site occupation. From the results (Table 3), it was clear that *G. edulis* recorded high K_F and $1/n_F$ values than *K. alvarezii*. This implies that binding capacity of *G. edulis* was the highest and the affinity between *G. edu-lis* biomass and CV was also high. However, the description of CV experimental data by the Freundlich model was not satisfactory as relatively low R^2 values were observed (Table 3). In an effort to enhance prediction of CV isotherm data, the Redlich–Peterson model (three-parameter) was used in the present study. This model combines the features of both the Langmuir and Freundlich model into a single equation and suggested the mechanism of adsorption as hybrid and does not follow ideal monolayer adsorption [33]. As expected, the Redlich–Peterson model described CV isotherm data with good accuracy (Table 3). All model constants were observed maximum for *G. edu-lis*. The Redlich–Peterson exponent was close to unity which confirms that CV isotherm was more of the Langmuir form. Furthermore, the Sips model was used to describe CV isotherms obtained for two red seaweeds. The Sips isotherm [34] is a combined form of the Langmuir and Freundlich equations, developed for the prediction of heterogeneous systems. The Sips model exponent (β_S) denotes the heterogeneity of the system, i.e. larger value of β_S implies high heterogeneity of the system. At low solute concentrations, the Sips model reduces to Freundlich form; while at high concentrations, it predicts the Langmuir model. Table 1 denotes that β_S values were closer or greater than unity; this indicates that the present system was more of Langmuir and heterogeneous. Application of the Sips model resulted in high

R^2 values for all isotherm data examined (Table 3). The isotherm curves as predicted by all four isotherm models examined are presented in Figs. 8 and 9.

4. Conclusions

The following conclusions can be summarized from the present study:

(1) The biosorption capacity of *G. edulis* and *K. alvarezii* strongly dependent upon sorbent particle size and dosage. Optimization experiments indicate that maximum CV uptake was achieved at 1.18 mm seaweed particle size and 5 g/L seaweed dosage.

(2) Solution pH strongly influenced biosorption capacity of *G. edulis* and *K. alvarezii* with pH 8 as an optimum for maximum removal of crystal violet.

(3) FT-IR and SEM analyses suggested a possible involvement of various functional groups with crystal violet molecules on the surfaces of red seaweeds.

(4) The rate of biosorption was found to be fast with and equilibrium was attained within 360 min. Application of CV kinetics data to the pseudo-first-order model resulted in good prediction compared to pseudo-second-order model.

(5) The maximum CV biosorption capacity was identified as 181.0 and 171.9 mg/g for *G. edulis* and *K. alvarezii*, respectively, according to the Langmuir model.

(6) From these results, it can be concluded that both red seaweeds showed high potential to act as an efficient and practical biosorbent for the removal of CV molecules from wastewater.

List of symbols

a_{RP}	—	Redlich–Peterson isotherm constant (L/mg$_{RP}^{\beta}$)
a_S	—	sips model coefficient (L/mg)$_S^\beta$
b_L	—	Langmuir equilibrium constant (L/mg)
C_0	—	initial dye concentrations (mg/L)
C_f	—	final dye concentrations (mg/L)
k_1	—	first-order equilibrium rate constant (min^{-1})
k_2	—	second-order equilibrium rate constant (g/mg min)
K_F	—	Freundlich constant (mg/g (L/mg))$^{1/n_F}$
K_{RP}	—	Redlich–Peterson isotherm constant (L/g)
K_S	—	sips model isotherm coefficient (L/g)$_S^\beta$
M	—	mass of biosorbents (g)
n_F	—	Freundlich exponent
Q	—	dye uptake (mg/g)
Q_{cal}	—	calculated dye uptake (mg/g)
Q_e	—	amount of dye biosorbed at anytime t (mg/g)
Q_{exp}	—	experimental dye uptake (mg/g)
Q_{max}	—	maximum dye uptake (mg/g)
V	—	volume of dye solution (L)
β_{RP}	—	Redlich–Peterson model exponent
β_S	—	sips model exponent

References

[1] Q. Zhang, T. Zhang, T.L. He, Removal of crystal violet by clay/PNIPAm nanocomposite hydrogels with various clay contents, Appl. Clay Sci. 90 (2014) 1–5.

[2] A. Saeed, M. Sharif, M. Iqbal, Application potential of grapefruit peel as dye sorbent: Kinetics, equilibrium and mechanism of crystal violet adsorption, J. Hazard. Mater. 179 (2010) 564–572.

[3] Y. Lin, X. He, G. Han, Q. Tian, Removal of Crystal Violet from aqueous solution using powdered mycelial biomass of *Ceriporia lacerata* P2, J. Environ. Sci. 23 (2011) 2055–2062.

[4] C.C. Chen, H.A. Liao, C.Y. Cheng, C.Y. Yen, Y.G. Chung, Biodegradation of crystal violet by *Pseudomonas putida*, Biotechnol. Lett. 29 (2007) 391–396.

[5] F. Zhou, Y. Cheng, L. Gan, Z. Chen, M. Megharaj, R. Naidu, *Burkholderia vietnamiensis* C09 V as the functional biomaterial used to remove crystal violet and Cu(II), Ecotoxicol. Environ. Saf. 105 (2014) 1–6.

[6] M.T. Yagub, T.K. Sen, S. Afroze, H.M. Ang, Dye and its removal from aqueous solution by adsorption: A review, Adv. Colloid Interface Sci. 209 (2014) 172–184.

[7] K. Vijayaraghavan, Y. Yun, Bacterial biosorbents and biosorption, Biotechnol. Adv. 26 (2008) 266–291.

[8] T.A. Khan, R. Rahman, I. Ali, E.A. Khan, A.A. Mukhlif, Removal of malachite green from aqueous solution using waste pea shells as low-cost adsorbent —Adsorption isotherms and dynamics, Toxicol. Environ. Chem. 96 (2014) 569–578.

[9] S. Li, M. Tao, Removal of cationic dyes from aqueous solutions by a biosorbent: Longan shell, Desalin. Water Treat. 57(11) (2016) 5193–5199.

[10] K. Vijayaraghavan, Y. Yun, Biosorption of C.I. Reactive Black 5 from aqueous solution using acid-treated biomass of brown seaweed *Laminaria sp*, Dyes Pigm. 76 (2008) 726–732.

[11] E. Daneshvar, M. Kousha, M.S. Sohrabi, A. Khataee, A. Converti, Biosorption of three acid dyes by the brown macroalga *Stoechospermum marginatum*: Isotherm, kinetic and thermodynamic studies, Chem. Eng. J. 195–196 (2012) 297–306.

[12] M. El Haddad, A. Regti, R. Slimani, S. Lazar, Assessment of the biosorption kinetic and thermodynamic for the removal of safranin dye from aqueous solutions using calcined mussel shells, J. Ind. Eng. Chem. 20 (2014) 717–724.

[13] K. Vijayaraghavan, K. Palanivelu, M. Velan, Biosorption of copper(II) and cobalt(II) from aqueous solutions by crab shell particles, Bioresour. Technol. 97 (2006) 1411–1419.

[14] N. Barka, M. Abdennouri, M.E. Makhfouk, S. Qourzal, Biosorption characteristics of cadmium and lead onto eco-friendly dried cactus (*Opuntia ficus indica*) cladodes, J. Environ. Chem. Eng. 1 (2013) 144–149.

[15] M. El Haddad, R. Mamouni, N. Saffaj, S. Lazar, Removal of a cationic dye—Basic Red 12—From aqueous solution by adsorption onto animal bone meal, J. Assoc. Arab Univ. Basic Appl. Sci. 12 (2012) 48–54.

[16] R. Slimani, I. El Ouahabi, F. Abidi, M. El Haddad, A. Regti, M.R. Laamari, S. El Antri, S. Lazar, Calcined eggshells as a new biosorbent to remove basic dye from aqueous solutions: Thermodynamics, kinetics, isotherms and error analysis, J. Taiwan Inst. Chem. Eng. 45 (2014) 1578–1587.

[17] J. Tangaromsuk, P. Pokethitiyook, M. Kruatrachue, E.S. Upatham, Cadmium biosorption by *Sphingomonas paucimobilis* biomass, Bioresour. Technol. 85 (2002) 103–105.

[18] J. Vijayaraghavan, T. Bhagavathi Pushpa, S.J. Sardhar Basha, K. Vijayaraghavan, J. Jegan, Evaluation of red marine alga *Kappaphycus alvarezii* as biosorbent for methylene blue: Isotherm, kinetic and mechanism studies, Sep. Sci. Technol. 50 (2015) 1–7.

[19] S. Li, M. Tao, Y. Xie, Reduced graphene oxide modified luffa sponge as a biocomposite adsorbent for effective removal of cationic dyes from aqueous solution, Desalin. Water Treat. (in press), doi: 10.1080/19443994.2015.1106344.

[20] I.D. Mall, V.C. Srivastava, G.V.A. Kumar, I.M. Mishra, Characterization and utilization of mesoporous fertilizer plant waste carbon for adsorptive removal of dyes from aqueous solution, Colloids Surf. A: Physicochem. Eng. Aspects 278 (2006) 175–187.

[21] V. Murphy, H. Hughes, P. McLoughlin, Enhancement strategies for Cu(II), Cr(III) and Cr(VI) remediation by a variety of seaweed species, J. Hazard. Mater. 166 (2009) 318–326.

[22] A.E. Navarro, R.F. Portales, M.N. Sun-Kou, B.P. Llanos, Effect of pH on phenol biosorption by marine seaweeds, J. Hazard. Mater. 156 (2008) 405–411.

[23] T.A. Khan, M. Nazir, E.A. Khan, Magnetically modified multiwalled carbon nanotubes for the adsorption of bismarck brown R and Cd(II) from aqueous solution: Batch and column studies, Desalin. Water Treat. (in press), doi: 10.1080/19443994.2015.1100553.

[24] I. Guerrero-Coronilla, L. Morales-Barrera, E. Cristiani-Urbina, Kinetic, isotherm and thermodynamic studies of amaranth dye biosorption from aqueous solution onto water *hyacinth leaves*, J. Environ. Manage. 152 (2015) 99–108.

[25] G. Limousin, J.P. Gaudet, L. Charlet, S. Szenknect, V. Barthès, M. Krimissa, Sorption isotherms: A review on physical bases, modeling and measurement, Appl. Geochem. 22 (2007) 249–275.

[26] I. Langmuir, The constitution and fundamental properties of solids and liquids, J. Am. Chem. Soc. 38 (1916) 2221–2295.

[27] T.A. Khan, S.A. Chaudhry, I. Ali, Equilibrium uptake, isotherm and kinetic studies of Cd(II) adsorption onto iron oxide activated red mud from aqueous solution, J. Mol. Liq. 202 (2015) 165–175.

[28] P.D. Saha, S. Chakraborty, S. Chowdhury, Batch and continuous (fixed-bed column) biosorption of crystal violet by *Artocarpus heterophyllus* (jackfruit) leaf powder, Colloids Surf. B: Biointerfaces 92 (2012) 262–270.

[29] T.A. Khan, E.A. Khan, Removal of basic dyes from aqueous solution by adsorption onto binary iron-manganese oxide coated kaolinite: Non-linear isotherm and kinetics modeling, Appl. Clay Sci. 107 (2015) 70–77.

[30] K. Vijayaraghavan, Y. Premkumar, J. Jegan, Malachite green and crystal violet biosorption onto coco-peat: Characterization and removal studies, Desalin. Water Treat. 57(14) (2016) 6423–6431.

[31] S. Neupane, S.T. Ramesh, R. Gandhimathi, P.V. Nidheesh, Pineapple leaf (*Ananas comosus*) powder as a biosorbent for the removal of crystal violet from aqueous solution, Desalin. Water Treat. 54 (2015) 2041–2054.

[32] H.M.F. Freundlich, About the adsorption in solution, Z. Phys. Chem. 57 (1906) 385–471.

[33] O. Redlich, D.L. Peterson, A useful adsorption isotherm, J. Phys. Chem. 63 (1959) 1024–1024.

[34] R. Sips, On the structure of a catalyst surface, J. Chem. Phys. 16 (1948) 490–495.